Direct enrichment of pathogens from physiological samples of high conductivity and viscosity using H-filter and positive dielectrophoresis

Dongyang Cai,[1,2] Qiaolian Yi,[1,3] Chaohua Shen,[1] Ying Lan,[1] Gerald Urban,[2] and Wenbin Du[1,4,a)]

[1]*State Key Laboratory of Microbial Resources, Institute of Microbiology, Chinese Academy of Sciences, Beijing 100101, China*
[2]*Laboratory for Sensors, Department of Microsystems Engineering - IMTEK, University of Freiburg, Freiburg 79110, Germany*
[3]*College of Life Sciences, University of the Chinese Academy of Sciences, Beijing 10049, China*
[4]*Savaid Medical School, University of the Chinese Academy of Sciences, Beijing 10049, China*

(Received 19 November 2017; accepted 9 January 2018; published online 23 January 2018)

The full potential of microfluidic techniques as rapid and accurate methods for the detection of disease-causing agents and foodborne pathogens is critically limited by the complex sample preparation process, which commonly comprises the enrichment of bacterial cells to detectable levels. In this manuscript, we describe a microfluidic device which integrates H-filter desalination with positive dielectrophoresis (pDEP) for direct enrichment of bacterial cells from physiological samples of high conductivity and viscosity, such as cow's milk and whole human blood. The device contained a winding channel in which electrolytes in the samples continuously diffused into deionized (DI) water (desalination), while the bacterial cells remained in the samples. The length of the main channel was optimized by numerical simulation and experimentally evaluated by the diffusion of fluorescein into DI water. The effects of another three factors on H-filter desalination were also investigated, including (a) the flow rate ratio between the sample and DI water, (b) sample viscosity, and (c) non-Newtonian fluids. After H-filter desalination, the samples were withdrawn into the dielectrophoresis chamber in which the bacterial cells were captured by pDEP. The feasibility of the device was demonstrated by the direct capture of the bacterial cells in 1× PBS buffer, cow's milk, and whole human blood after H-filter desalination, with the capture efficiencies of 70.7%, 90.0%, and 80.2%, respectively. We believe that this simple method can be easily integrated into portable microfluidic diagnosis devices for rapid and accurate detection of disease-causing agents and foodborne pathogens. *Published by AIP Publishing.* https://doi.org/10.1063/1.5016413

I. INTRODUCTION

Rapid and accurate detection of disease-causing agents and foodborne pathogens is crucial for timely treatment with appropriate antimicrobials and precautionary measures to maintain healthy food.[1,2] One of the inherent difficulties in detecting these microorganisms is their extremely low abundance in the samples. For example, the concentration of bacterial cells in bloodstream may be as low as 1 to 10 CFU/ml in the early stage of sepsis and that of foodborne pathogens in food matrices may be lower than 100 CFU/g with the presence of millions of non-pathogenic cells.[3,4] Conventional culture-based methods for detecting these pathogens

a)Author to whom correspondence should be addressed: wenbin@im.ac.cn

include preparation of culture media, long-term incubation, inoculation of plates, and overnight subculture, which are laborious and time-consuming.[1,4] Moreover, the majority of these steps are performed in centralized laboratories using instrumentation that requires high-infrastructure support and highly trained laboratory technicians and therefore limits their employment in resource-limited settings.[2,5]

Microfluidic techniques have become increasingly prominent in high efficient separation and analysis for various biomedical applications.[6–8] Researchers from both academia and industry are interested in developing portable microfluidic systems to provide rapid, inexpensive, and efficient point-of-care diagnostic solutions. However, a major bottleneck of these systems for detecting disease-causing agents and foodborne pathogens is the complex sample preparation process which commonly requires the enrichment of bacterial cells to detectable levels.[9,10] Various microfluidic-based approaches for the enrichment of bacterial cells have been developed, including membrane filtration,[11] immunomagnetic capture,[12] optical trapping,[13] and acoustophoretic separation.[14] However, these techniques are still limited by complex system configurations, the requirement of pre-labelling, and the insufficiency to capture bacterial or fungal cells with different sizes.

Dielectrophoresis (DEP) is the electrokinetic motion of dielectrically polarized particles in non-uniform electric fields.[15] Microfluidic-based DEP enables selective and label-free transport, capture, and enrichment of microbial cells from physiological samples,[16,17] which is essential for the detection of pathogens from complex matrices. It provides several advantages over conventional techniques, including target specific control without pre-labelling, electric field manipulation without moving parts, and ease of integration with other components on portable microfluidic devices.[9] Polarized bacterial cells can be attracted to the region of electric-field maximum (positive DEP, pDEP) or repelled to the region of electric-field minimum (negative DEP, nDEP) depending on their polarizability with respect to the surrounding medium. In pDEP, target cells in a continuous sample flow can be selectively captured near the electrodes, while non-target particles are continuously carried out of the device by the flow. The captured target cells then can be released and collected at the outlet of the device by turning off the supplied electric power. Therefore, pDEP has been widely applied for sample enrichment to improve sensitivity and reduce assay time.[17]

A main drawback of pDEP is the requirement of sample media with low conductivity, such as deionized (DI) water or sucrose solution.[18,19] Unfortunately, most clinical samples and food matrices, such as whole human blood and cow's milk, have high conductivity. Bacterial cells become less polarizable in these samples, resulting in ineffective pDEP.[20,21] Therefore, the employment of pDEP in a continuous sample flow of high conductivity is limited only when the conductivity can be reduced.

To reduce the conductivity of samples, ion-exchange membranes have been fabricated in microfluidic systems for the ion concentration or depletion with a spatially inhomogeneous ion concentration distribution in microfluidic devices.[22–24] However, it remains challenging to design and integrate ion-selective membranes on microfluidic devices for a continuous process of a large amount of samples. An alternative to the ion-exchange membrane method is using a membraneless H-filter, which allows continuous separation of small molecules with high diffusion coefficients from other components of the sample with low diffusion coefficients.[25,26] Two separate flows (a sample flow and a DI water flow) are brought together to flow alongside each other in a main channel. The laminar flow conditions found in microfluidic devices minimize convective mixing between the adjacent flows, and thus, molecules from one flow move to another flow only *via* diffusion. The employment of the H-filter for the isolation of small analytes from filtered saliva samples and cephradine (a semisynthetic cephalosporin antibiotic) from blood samples has been reported.[27,28] Very recently, membraneless microdialysis devices (MMDs) with the H-filter design have been reported which effectively enhanced the capture of bacterial cells from whole human blood by pDEP.[29] In that work, a cascaded connection of multiple MMDs was used to deplete ions in blood to 100-fold below physiological levels. However, the cascaded structure caused difficulties in assembly and loss of cells, as indicated by the obtained recovery rate of 78.2%–79.5%. Whether integration of a single step H-filter with pDEP can sufficiently capture bacterial cells from physiological samples remains unclear. Moreover, most physiological

samples including whole human blood are highly viscous and may have viscoelastic and shear thinning properties.[30,31] Whether these properties will affect H-filter desalination and the recovery of bacterial cells has not been investigated yet.

In this manuscript, we describe a fully integrated microfluidic device which couples H-filter desalination with pDEP capture for direct enrichment of bacterial cells from physiological samples of high conductivity and viscosity. The H-filter comprised a long and winding channel for high efficient desalination of the samples, and the interdigitated microelectrodes with small spacing were used to effectively enrich the bacterial cells from the samples after H-filter desalination. With this device, bacterial cells in physiological samples of high conductivity and viscosity can be directly enriched by pDEP without conductivity adjustment prior to the sample analysis. The feasibility of the device was demonstrated by the enrichment of bacterial cells from 1× phosphate-buffered saline (PBS) buffer, cow's milk, and whole human blood after H-filter desalination, with high capture efficiencies of 70.7%, 90.0%, and 80.2%, respectively.

II. EXPERIMENTAL

A. Sample preparation

A solution of 200 mM fluorescein (Sigma-Aldrich, St. Louis, MO, USA) was prepared in 1× PBS buffer (pH = 7.0). Solutions of 200 mM fluorescein containing 20%, 35%, 50%, and 65% w/v sucrose (Sigma-Aldrich) or 0.1% w/v Xanthan gum (XG) (Sigma-Aldrich) were prepared in 1× PBS buffer (pH = 7.0), respectively.

Escherichia coli (*E. coli*) RP437 was provided by Professor J. S. Parkinson from the University of Utah and transformed with DsRedT.4 plasmid (Clontech Laboratories, Mountain View, CA). A single colony of *E. coli* RP437 on the Luria-Bertani (LB) agar plate was inoculated into 5 ml LB broth and then cultured overnight. A subculture was prepared in 5 ml fresh LB broth and shaken at 37 °C for 5 h.

EDTA-treated blood samples were obtained from the Hospital of Renmin University of China and stored at 4 °C before use. Informed consent was obtained from all blood donors, and the study was approved by the Hospital of Renmin University of China Ethics Board. Cow's milk (conventionally and organically produced) was purchased from the same supermarket in Renmin University of China. 10 μl LB broth with bacterial cells of *E. coli* RP437 was separately spiked into 1 ml blood and cow's milk with a concentration of $\sim 2 \times 10^7$ CFU/ml. The addition of 1% Bovine Albumin Serum (BSA, Sigma-Aldrich) was used to prevent the adhesion of cells on the microchannel walls.

B. Device fabrication and assembly

The top polydimethylsiloxane (PDMS) layer containing a winding channel (37 cm in length, 500 μm in width, and 22 μm in depth) was fabricated by standard photolithography. Access holes were punched to make inlets and outlets of the channel using a sharpened 21-gauge needle. The bottom plate was made of a 1 mm thick glass with indium tin oxide (ITO) coating by standard photolithography and wet etching techniques.[16] The ITO layer was etched to make an interdigitated ITO microelectrode array (2000 μm in length, 35 μm in width, and 25 μm in spacing) for DEP capture. The top PDMS layer and the bottom ITO layer were aligned and bonded by oxygen plasma treatment with the microelectrode array locating in the center of the DEP chamber.

Electrical wires were adhered to the microelectrodes by conductive tapes to supply AC power which was generated by a function generator up to 20 MHz frequency. Four 250 μl syringes (Agilent, Santa Clara, CA) were connected to the device through 30-gauge Teflon tubing (Weico Wire &Cable, Edge-wood, NY). Syringe pumps (Pump 11, PicoPlus Elite, Harvard Apparatus, Holliston, MA, USA) were used for the infusion and suction of the samples and DI water.

C. Device operation

The samples were infused into the device at a flow rate of 0.5 μl/min from the sample inlet, and DI water was infused into the device at a flow rate of 5 μl/min (optimized flow rate) from

the DI water inlet. These two inlets converged into a main channel and then split into a DEP chamber and a waste channel [Fig. 1(a)]. In the main channel, the electrolytes in the samples continuously diffused into DI water. After H-filter desalination, the samples were withdrawn into the DEP chamber at a flow rate of 1 μl/min to avoid the loss of target cells. Meanwhile, DI water was withdrawn into the waste channel at a flow rate of 4.5 μl/min. In the DEP chamber, the bacterial cells in the desalinated samples were captured by pDEP when a high frequency alternating current signal of 20 Vpp (peak-to-peak voltage) and 20 MHz was applied between the interdigitated microelectrodes [Fig. 1(b)]. During the experiments, the diffusion of fluorescein and motions of RFP-tagged *E. coli* RP437 were observed by using an Eclipse Ti inversed microscope (Nikon, Japan) with a CoolSNAP HQ2 CCD camera (Photometrics, Tucson, AZ). The capture efficiency of the device was calculated as follows: microscopic fluorescence images were taken in the channel prior to and after the DEP chamber; the cell number in each image was counted to calculate the DEP capture efficiency. Three independent experiments were performed to calculate the capture efficiency and the recovery rate of bacterial cells.

D. Numerical simulation

The diffusion of fluorescein in the main channel was stimulated by COMSOL Multiphysics (COMSOL Inc., Burlington, MA, USA). The diffusion coefficient of fluorescein (MW 372) in water of 4.9×10^{-6} cm^2/s was used.[32]

III. RESULTS AND DISCUSSION

A. Evaluation of diffusion in the main channel

In the H-filter, the time spent flowing in the main channel is proportional to its length, and thus, an appropriate length of the main channel allows for controlled isolation of electrolytes with high diffusion coefficients from other components of the samples with low diffusion coefficients. To optimize the length of the main channel, COMSOL was used to simulate the diffusion of fluorescein in the parallel flows. Herein, the fluorescein solution and DI water were

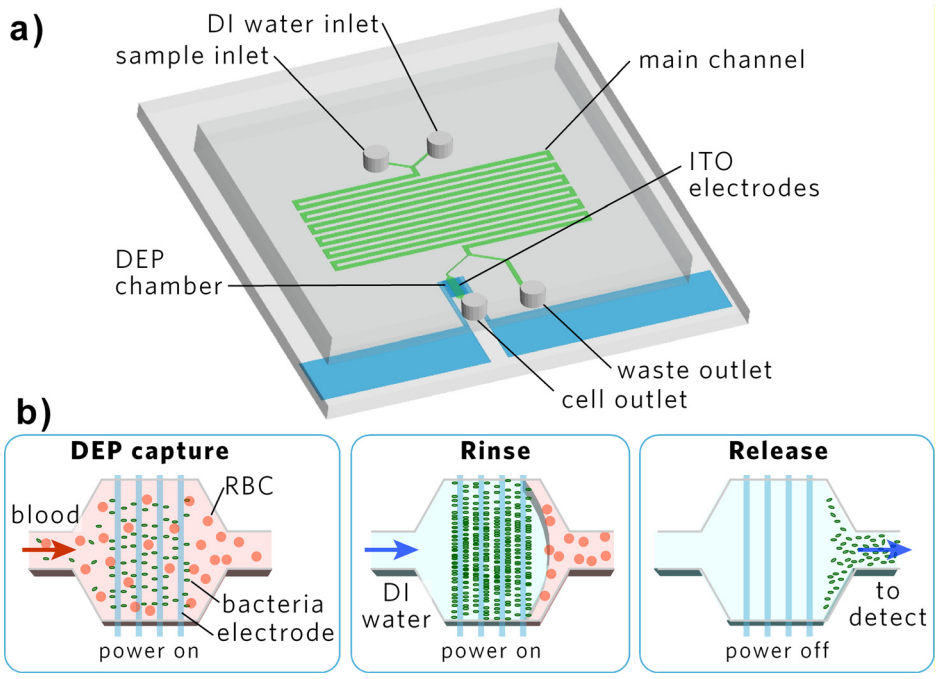

FIG. 1. (a) Schematic illustration of the device which integrated H-filter desalination and pDEP capture and (b) pDEP capture of bacterial cells after H-filter desalination, including DEP capture, rinse to remove any residues, and DEP release to collect the bacterial cells in the DEP chamber for off-line analysis.

infused into the main channel at flow rates of 0.5 μl/min and 1 μl/min, respectively. The numerical simulation of the diffusion in the main channel and zoomed-in views of upstream and downstream are shown in Figs. 2(a)–2(c). At upstream of the main channel, a narrow and steep step of fluorescence between fluorescein solution and DI water was observed [Fig. 2(b)]. As the diffusion carrying out along the main channel, the fluorescein continuously diffused into DI water and the gradient vanished at downstream of the main channel [Fig. 2(c)]. Next, we performed experiments following the same conditions, using 200 mM fluorescein in 1× PBS buffer. The theoretical and experimental results at upstream and downstream of the main channel were compared and showed a great similarity [Figs. 2(b)–2(e)]. Line scans were drawn across the center of 11 horizontal sections of the main channel [Figs. 2(a) and 2(f)]. The fluorescence intensity curve originating from the line scans is shown in Fig. 2(g). It was found that the fluorescence intensities across the center of sections 10 and 11 were similar, indicating the adequate length of the main channel for the diffusion of 200 mM fluorescein under current experimental conditions.

B. Effects of flow rate ratio on H-filter diffusion

The flow rate ratio between the fluorescein solution and DI water was optimized to obtain better diffusion. The flow rate of 200 mM fluorescein was fixed at 0.5 μl/min. A higher flow rate of DI water leads to a narrower flow of the fluorescein solution, resulting in a shorter diffusion distance of fluorescein. Moreover, a higher flow rate of DI water generates a larger concentration gradient between fluorescein solution and DI water, producing higher rates of diffusion and dilution. DI water was infused into the main channel at flow rates of 0.5, 1, 2.5, and 5 μl/min. Fluorescence intensity profiles originating from the line scans at upstream and downstream of the main channel are demonstrated [Figs. 3(a) and 3(b)]. It was found that the higher flow rate of DI water was used, the better diffusion could be obtained. The flow rate of fluorescein solution at 0.5 μl/min and the flow rate of DI water at 5 μl/min were used in the following

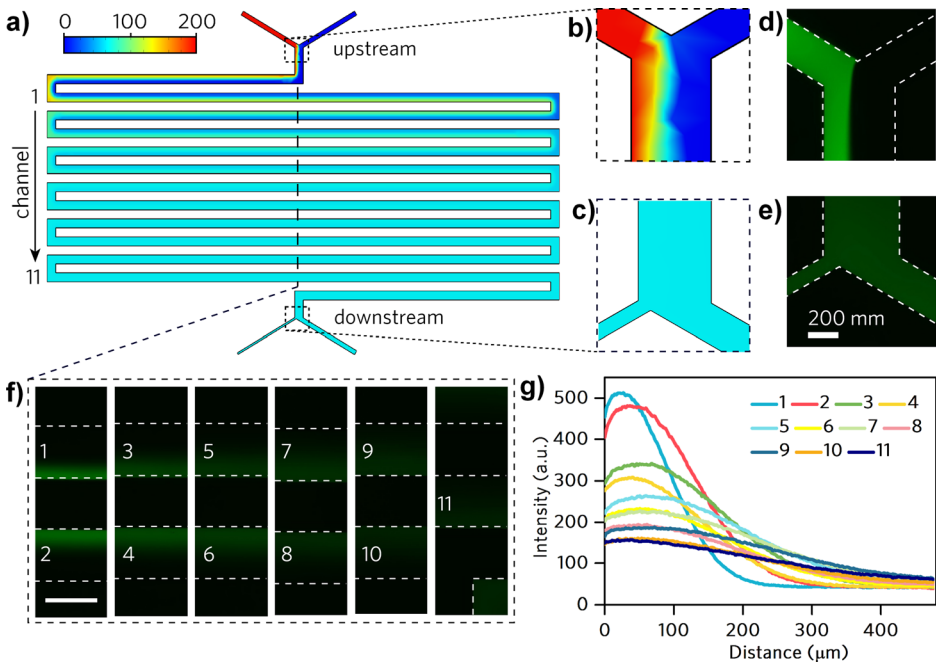

FIG. 2. Evaluation of diffusion efficiency. The fluorescein solution and DI water were infused into the main channel (37 cm in length, 500 μm in width, and 22 μm in depth) at flow rates of 0.5 μl/min and 1 μl/min. (a) Numerical stimulation of the diffusion of fluorescein (200 mM) in the main channel of the H-filter. (b)–(e) Numerical simulation and experimental results of fluorescein diffusion at upstream and downstream of the main channel. (f) Fluorescence images at the center of 11 horizontal sections of the main channel. (g) Fluorescence intensity curve originating from the line scans at the center of 11 horizontal sections of the main channel.

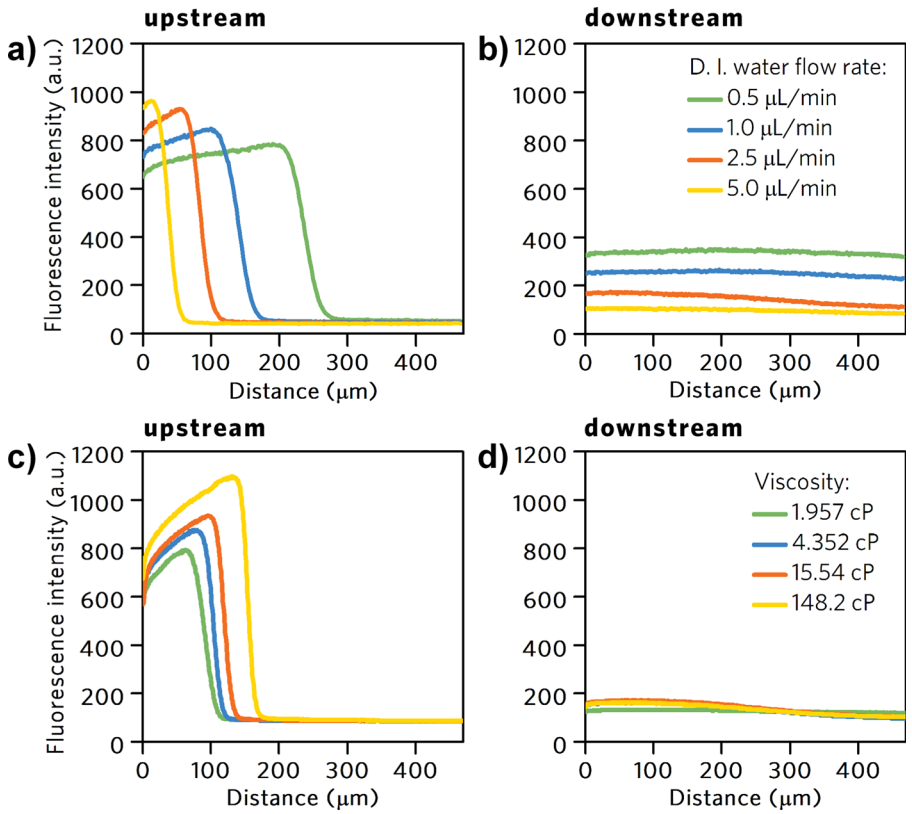

FIG. 3. Effects of the flow rate ratio and viscosity on H-filter diffusion illustrated by fluorescence intensity profiles originating from the line scans at upstream and downstream of the main channel. (a) and (b) The flow rate of fluorescein solution was fixed at 0.5 μl/min, and the flow rates of DI water were changing from 0.5 to 5 μl/min. (c) and (d) The viscosity of the fluorescein solution was adjusted to 1.957, 4.352, 15.54, and 148.2 cP by addition of sucrose. The fluorescein solution and DI water were infused into the main channel with flow rates of 0.5 μl/min and 5 μl/min, respectively.

experiments. In this situation, the fluorescein solution was withdrawn into the DEP chamber at a flow rate of 1 μl/min and the DI water was withdrawn into the waste channel at a flow rate of 4.5 μl/min, with consideration of bacterial motility. Under this condition, the highest desalination efficiency we could obtain is around 10 folds. Whether it is sufficient to enhance bacterial cell capture by pDEP from physiological samples will be discussed later (Fig. 6).

C. Effects of sample viscosity on H-filter diffusion

Most physiological samples have a higher viscosity than water. The sample viscosity can dramatically influence its occupation across the width of the main channel. In the case of two samples with equivalent viscosity flowing at the same flow rate, each occupies equal fractions of the channel width. However, when two samples with different viscosities flowing at the same flow rate, the sample with a higher viscosity moves more slowly and occupies a greater fraction of the channel width, resulting in a long diffusion distance. Moreover, higher viscosity leads to a smaller diffusion coefficient according to the Stokes-Einstein equation

$$D = \frac{k_B T}{6\pi\eta r},$$

where D is the diffusion coefficient, k_B is Boltzmann's constant, T is the Kelvin temperature, r is the radius of the particles, and η is the viscosity of the sample. The viscosities of the sucrose-fluorescein solutions prepared in Sec. II were 1.957, 4.352, 15.54, and 148.2 cP at 20 °C.[33] The sucrose-fluorescein solutions and DI water were infused into the main channel

with the optimized flow rates. Fluorescence intensity curves originating from the line scans at upstream and downstream of the main channel are demonstrated [Figs. 3(c) and 3(d)]. At upstream, the sample with higher viscosity occupied a greater fraction of the channel width. It was also found that the sample with higher viscosity showed a higher fluorescence intensity. This is because the increased sample viscosity reduces the molecular collision opportunity, resulting in reduced radiationless transition.[34] At downstream, the fluorescence intensity curves of the samples with different viscosities showed a great similarity, indicating the capacity of the H-filter to deal with samples with different viscosities.

D. Effect of non-Newtonian fluids on H-filter diffusion

Fluorescein solution with Xanthan gum (XG) was used to evaluate the performance of the H-filter for processing non-Newtonian physiological fluids.[35] 0.1% XG-fluorescein solution and DI water were infused into the main channel with the optimized flow rates. It was found that the XG-fluorescein solution occupied a greater fraction of the channel width as expected because of its high viscosity. It was also found that the interface between the XG-fluorescein solution and DI water was both curved and unstable [Fig. 4(b)]. This phenomenon was previously reported as the result of different viscosities and elasticity stratifications between the parallel fluids.[35] Fluorescence intensity curves originating from the line scans at upstream and downstream of the main channel are shown in Fig. 4(c). 200 mM fluorescein solution was used as the control sample. At downstream, the fluorescence intensity curves originating from XG-fluorescein solution and 200 mM fluorescein solution showed a great similarity, indicating the capacity of the H-filter to deal with samples of non-Newtonian fluids.

E. Loss of bacterial cells due to the viscoelastic properties of physiological samples

To investigate whether the viscoelastic properties of physiological samples will affect bacterial cell recovery during H-filter desalination, we performed H-filtration of the bacterial

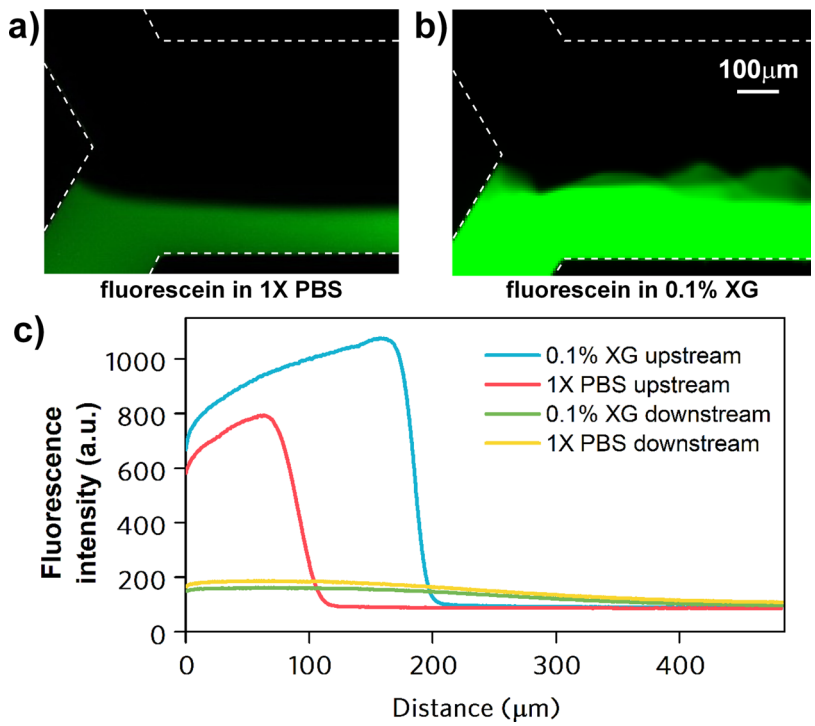

FIG. 4. Effect of non-Newtonian fluids on H-filter diffusion. (a) and (b) Fluorescence images show upstream parallel flow of 200 mM fluorescein and DI water. Fluorescein is dissolved in (a) 1× PBS and (b) 1× PBS with 0.1% Xanthan Gum (XG). (c) Fluorescence intensity profiles perpendicular to the direction of flow from upstream and downstream.

suspension in 1× PBS, cow's milk, and whole human blood using the optimized conditions as described above and imaged both upstream and downstream of the main channel [Figs. 5(a)–5(f)]. These samples were infused into the device at a flow rate of 0.5 μl/min and withdrawn into the DEP chamber at a flow rate of 1 μL/min to avoid the loss of bacterial cells. The merged images of fluorescence and bright-field showed that the increased withdraw flow rate was sufficient for complete recovery of bacterial cells from 1× PBS with a recovery rate of 99.8% [Fig. 5(g)]. However, the viscoelastic properties of cow's milk and whole human blood led to increased occupation of the channel width at both upstream and downstream, and the recovery rate decreased to 90.1% and 67.0% for cow's milk and whole human blood, respectively [Fig. 5(g)]. These results confirm that we should take account of the viscoelastic properties of target samples during designing H-filter desalination. To avoid the loss of bacterial cells during H-filtration, we can increase either the fraction of the channel width or the withdraw flow rate allocated to the DEP chamber.

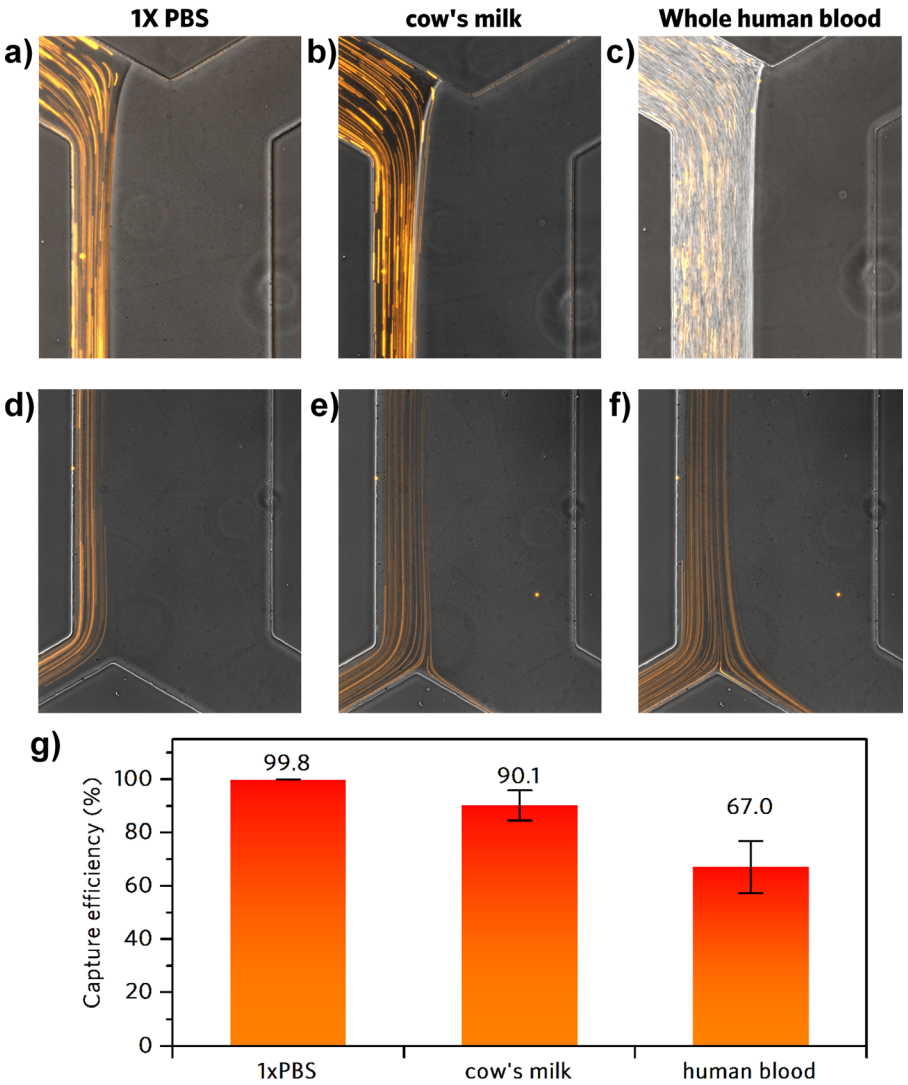

FIG. 5. (a)–(f) Microscopic images showing the recovery of bacterial cells from 1× PBS, cow's milk, and whole human blood after H-filter desalination. The occupancy of the channel width at upstream and downstream of the main channel is different for 1× PBS (a) and (d), cow's milk (b) and (e), and whole human blood (c) and (f) due to their different viscoelastic properties; the images were created by merging the RFP channel and the bright-field channel. (g) Recovery rate of bacterial cells from 1× PBS, cow's milk, and whole human blood after H-filter desalination.

F. Direct capture of bacterial cells from physiological samples by pDEP

To confirm the negative effect of high solution conductivity on the pDEP capture of bacterial cells, we carried out control experiments without H-filter processing using samples of different conductivities. DI water, 0.1× PBS buffer (1.7 mS/cm, 20 °C), and 1× PBS buffer (13.6 mS/cm, 20 °C) spiked with $\sim 2 \times 10^7$ CFU/ml RFP-tagged *E. coli* RP437 were directly infused into the DEP chamber at a flow rate of 1 μl/min. When a high frequency alternating current signal of 20 Vpp and 20 MHz was applied between the interdigitated microelectrodes, the bacterial cells spiked in DI water and 0.1× PBS buffer were captured by pDEP onto the edge of the microelectrodes with capture efficiencies of 99.8% and 57.5%, respectively [Figs. 6(a) and 6(c)]. However, the bacterial cells spiked in 1× PBS buffer cannot be captured due to its high conductivity [Figs. 6(a) and 6(c)].

To demonstrate the effectiveness of desalination, we tested if pDEP can capture bacterial cells from samples of high conductivity after H-filter processing. For 1× PBS solution with $\sim 2 \times 10^7$ CFU/ml *E. coli* RP437, a capture efficiency of 70.7% was obtained [Figs. 6(b) and

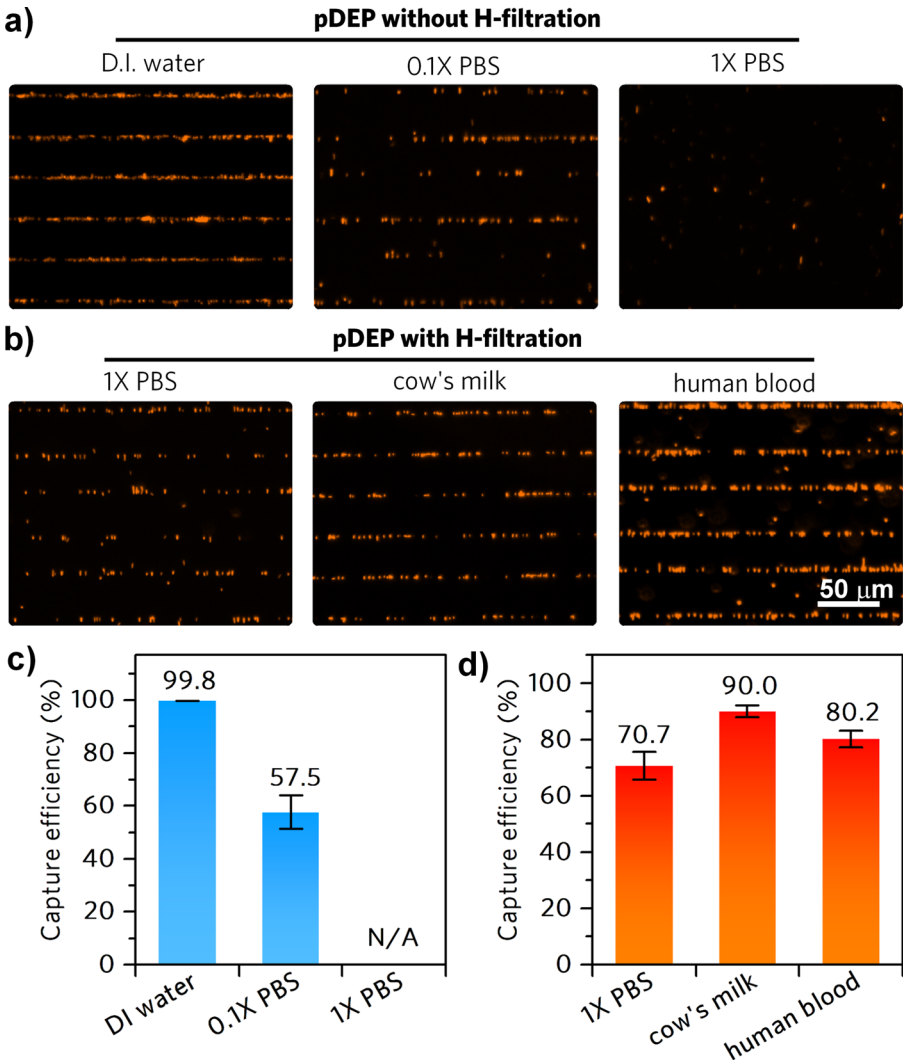

FIG. 6. (a) and (c) Fluorescence images and capture efficiency of the pDEP capture of bacterial cells after H-filter desalination. RFP-tagged RP437 spiked in water, 0.1× PBS buffer, and 1× PBS buffer were directly infused into the DEP chamber to test if the microelectrodes can capture the cells, respectively. No capture of cells was observed for 1× PBS. (b) and (d) pDEP capture of *E. coli* RP437 spiked in 1× PBS buffer, cow's milk, and human blood with the help of H-filter desalination. Error bars: SD of three independent experiments.

6(d)]. The feasibility of the device was further demonstrated with cow's milk (4.2 mS/cm, 20 °C) and whole human blood (6.7 mS/cm, 20 °C) spiked with $\sim 2 \times 10^7$ CFU/ml *E. coli* RP437. After H-filter desalination, the bacterial cells spiked in cow's milk and whole human blood were captured by pDEP onto the edge of the microelectrodes with capture efficiencies of 90.0% and 80.2%, respectively [Figs. 6(b) and 6(d)].

Red blood cells are much more osmotically fragile compared with bacterial cells. The H-filter treatment exposed the cells to osmotic stress and shear stress, which resulted in hemolysis of the red blood cells. The long and winding main channel design greatly increased the hemolysis efficiency, as indicated by the downstream image [Fig. 5(f)] compared to upstream image [Fig. 5(c)], in which the pale shades from red blood cells faded, and the fluorescence traces of RFP-tagged *E. coli* RP437 became clearer.

IV. CONCLUSIONS

Rapid and accurate detection of disease-causing agents and foodborne pathogens using microfluidic devices is critically limited by the complex sample preparation process which commonly comprises the enrichment of bacterial cells to detectable levels. In this manuscript, we describe a microfluidic device which integrates H-filter desalination with pDEP capture for direct enrichment of bacterial cells from physiological samples of high conductivity and viscosity. In the main channel of the H-filter, the electrolytes continuously diffused into DI water, while the bacterial cells remained in the samples. After desalination, the samples were withdrawn into the DEP chamber in which the bacterial cells were captured by pDEP. The feasibility of the device was demonstrated with 1× PBS, cow's milk, and whole human blood spiked with bacterial cells.

A very recent reported work has used cascaded connection of two MMD devices (using the H-filter structure) to realize 100-fold desalination of blood samples and to connect with another DEP capture device to capture bacterial cells.[29] Compared with that work, this independent research has the following unique features: (1) H-filter desalination was integrated with a pDEP capture unit on a single device; (2) for the blood sample, the long and winding channel exerted prolonged osmotic and shear stress to human blood cells, which resulted in effective hemolysis; (3) no permeabilizing agents were needed to alter the dielectrophoretic behavior of blood cells to realize the selective capture of bacterial cells by pDEP; (4) instead of using 100-fold desalination which requires cascaded connection of two H-filter devices and pDEP using 1 MHz and 15–20 Vpp signals, we used a different pDEP signal (20 MHz, 20 Vpp) which effectively and selectively capture bacterial cells with the maximum 11-fold desalination.

The described microfluidic device overcomes the limitation of pDEP which must be operated in the medium of low conductivity, therefore allowing the direct analysis of crude physiological samples without conductivity adjustment. The fabrication and manipulation of the device are quite simple. Importantly, we investigated the effect of sample viscosity and non-Newtonian fluids on H-filter desalination, which is critical for improving the capture efficiency and the recovery rate of bacterial cells from physiological samples. These unique characteristics will allow the method to be easily integrated into sample-to-answer devices for point-of-care testing and continuous monitoring of pathogens in clinical diagnostics, food safety testing, and environmental monitoring.

Microfluidic devices using 3D nDEP and 3D travelling wave DEP for the separation of bacterial cells and blood cells have been reported with higher throughput compared with our device.[36–38] Our future work will be directed towards developing microfluidic devices which integrate H-filter desalination with 3D pDEP capture for improved throughput to meet practical applications.

ACKNOWLEDGMENTS

This study was supported by the National Natural Science Foundation of China (31470221), Beijing Municipal Science & Technology Commission (Z161100000116042), the National Key Research and Development Program of China (2016YFC0100904, 2016YFE0205800), the Key

Program of Frontier Sciences of the Chinese Academy of Sciences (QYZDB-SSW-SMC008), the Key Research Program of the Chinese Academy of Sciences (KFZD-SW-219), and the Open Research Fund of State Key Laboratory of Bioelectronics, Southeast University.

[1]P. Tissari, A. Zumla, E. Tarkka, S. Mero, L. Savolainen, M. Vaara, A. Aittakorpi, S. Laakso, M. Lindfors, H. Piiparinen, M. Maki, C. Carder, J. Huggett, and V. Gant, Lancet **375**, 224–230 (2010).
[2]P. K. Mandal, A. K. Biswas, K. Choi, and U. K. Pal, Am. J. Food Technol. **6**, 87–102 (2011).
[3]J. A. Kellogg, J. P. Manzella, and D. A. Bankert, J. Clin. Microbiol. **38**, 2181–2185 (2000), see http://jcm.asm.org/content/38/6/2181.full.
[4]X. Zhao, C. W. Lin, J. Wang, and D. H. Oh, J. Microbiol. Biotechnol. **24**, 297–312 (2014).
[5]M. Urdea, L. A. Penny, S. S. Olmsted, M. Y. Giovanni, P. Kaspar, A. Shepherd, P. Wilson, C. A. Dahl, S. Buchsbaum, G. Moeller, and B. D. Hay, Nature **444**(1), 73–79 (2006).
[6]D. Mark, S. Haeberle, G. Roth, F. von Stetten, and R. Zengerle, Chem. Soc. Rev. **39**, 1153–1182 (2010).
[7]L. Zhang, B. Ding, Q. Chen, Q. Feng, L. Lin, and J. Sun, TrAC, Trends Anal. Chem. **94**, 106–116 (2017).
[8]J. Wu, Q. Chen, and J. M. Lin, Analyst **142**, 421–441 (2017).
[9]S. Park, Y. Zhang, T. H. Wang, and S. Yang, Lab Chip **11**, 2893–2900 (2011).
[10]I. H. Cho, L. Mauer, and J. Irudayaraj, Biosens. Bioelectron. **57**, 143–148 (2014).
[11]S. M. Kim, S. H. Lee, and K. Y. Suh, Lab Chip **8**, 1015–1023 (2008).
[12]M. A. Gijs, F. Lacharme, and U. Lehmann, Chem. Rev. **110**, 1518–1563 (2010).
[13]K. Dholakia, P. Reece, and M. Gu, Chem. Soc. Rev. **37**, 42–55 (2008).
[14]F. Petersson, L. Aberg, A. M. Sward-Nilsson, and T. Laurell, Anal. Chem. **79**, 5117–5123 (2007).
[15]H. A. Pohl, J. Appl. Phys. **29**, 1182–1188 (1958).
[16]D. Cai, M. Xiao, P. Xu, Y. C. Xu, and W. Du, Lab Chip **14**, 3917–3924 (2014).
[17]R. E. Fernandez, A. Rohani, V. Farmehini, and N. S. Swami, Anal. Chim. Acta **966**, 11–33 (2017).
[18]B. H. Lapizco-Encinas, B. A. Simmons, E. B. Cummings, and Y. Fintschenko, Anal. Chem. **76**, 1571–1579 (2004).
[19]L. Wu, Y. L. Lanry, and K. M. Lim, Biomicrofluidics **6**, 14113 (2012).
[20]S. H. Liao, C. Y. Chang, and H. C. Chang, Biomicrofluidics **7**, 24110 (2013).
[21]M. Koklu, S. Park, S. D. Pillai, and A. Beskok, Biomicrofluidics **4**, 034107 (2010).
[22]G. Sun, Z. Pan, S. Senapati, and H. Chang, Phys. Rev. Appl. **7**, 064024 (2017).
[23]Z. Slouka, S. Senapati, and H. C. Chang, Annu. Rev. Anal. Chem. **7**, 317–335 (2014).
[24]K. Zhou, M. L. Kovarik, and S. C. Jacobson, J. Am. Chem. Soc. **130**, 8614–8616 (2008).
[25]J. P. Brody, P. Yager, R. E. Goldstein, and R. H. Austin, Biophys. J. **71**, 3430–3441 (1996).
[26]J. P. Brody and P. Yager, Sens. Actuators, A **58**, 13–18 (1997).
[27]K. L. Helton, K. E. Nelson, E. Fu, and P. Yager, Lab Chip **8**, 1847–1851 (2008).
[28]P. Jandik, B. H. Weigl, N. Kessler, J. Cheng, C. J. Morris, T. Schulte, and N. Avdalovic, J. Chromatogr. A **954**, 33–40 (2002).
[29]L. D'Amico, N. J. Ajami, J. A. Adachi, P. R. Gascoyne, and J. F. Petrosino, Lab Chip **17**, 1340–1348 (2017).
[30]F. J. Gijsen, F. N. van de Vosse, and J. D. Janssen, J. Biomech. **32**, 601–608 (1999).
[31]F. Tian, W. Zhang, L. Cai, S. Li, G. Hu, Y. Cong, C. Liu, T. Li, and J. Sun, Lab Chip **17**, 3078–3085 (2017).
[32]W. Du, Q. Fang, and Z. Fang, Anal. Chem. **78**, 6404–6410 (2006).
[33]P. Honig, *Principles of Sugar Technology*, 1st ed. (Elsevier, 1953).
[34]G. Oster and Y. Nishijima, J. Am. Chem. Soc. **78**, 1581–1584 (1956).
[35]K. L. Helton and P. Yager, Lab Chip **7**, 1581–1588 (2007).
[36]R. S. Kuczenski, H. C. Chang, and A. Revzin, Biomicrofluidics **5**, 32005 (2011).
[37]R. Pethig, Biomicrofluidics **4**, 022701 (2010).
[38]S. A. Faraghat, K. F. Hoettges, M. K. Steinbach, D. R. van der Veen, W. J. Brackenbury, E. A. Henslee, F. H. Labeed, and M. P. Hughes, Proc. Natl. Acad. Sci. U.S.A. **114**, 4591–4596 (2017).